Classification
Physics Abstracts
4.375

(^{3}He, xn), (^{3}He, pxn) AND (^{3}He, FISSION) REACTIONS ON ^{206}Pb BETWEEN 80 AND 200 MeV

CH. ANDRE, H. GAUVIN and Y. LE BEYEC

Laboratoire de Chimie Nucléaire,
Institut de Physique Nucléaire, 91406 Orsay, France
and
N. T. PORILE (*)

Department of Chemistry, Purdue University,
Lafayette, Indiana 47907, U.S.A.

(*Reçu le 7 juillet 1975, révisé et accepté le 11 septembre 1975*)

Résumé. — Les réactions induites par des particules ^{3}He sur une cible de ^{206}Pb ont été étudiées entre 80 et 200 MeV. Les fonctions d'excitation (^{3}He, xn) pour $x = 3$ à 14 et (^{3}He, pxn) pour $x = 2$ à 5 ont été obtenues ainsi que les distributions angulaires des fragments de fission et les sections efficaces totales de fission à 100, 125, 150 et 175 MeV.

Une analyse des résultats est faite pour dégager les caractéristiques principales des mécanismes de réaction. L'ensemble de ces résultats montre que la contribution des processus non composés est prépondérante. Ceci est mis en évidence par l'émission très importante de particules chargées ainsi que par la distribution angulaire des fragments de fission proche de l'isotropie dans le système du laboratoire.

Dans le domaine d'énergie 25 à 45 MeV/nucléon, une comparaison est faite avec une étude expérimentale des réactions induites dans la même cible ^{206}Pb par des particules α ainsi qu'avec un modèle de collision α-noyau appliqué à ce système ^{206}Pb + α. Ces comparaisons et les observations suggèrent fortement une rupture de la particule incidente ^{3}He suivie des interactions du ou des fragments avec ^{206}Pb.

Abstract. — The reactions induced in ^{206}Pb by ^{3}He particles having energies between 80 and 200 MeV have been studied. Excitation functions for (^{3}He, xn) with $x = 3$ to 14 and for (^{3}He, pxn) with $x = 2$ to 5 have been obtained. Angular distributions of fission fragments were measured at 100, 125, 150 and 175 MeV and total fission cross-sections were deduced from the data.

On the basis of these results, analysis is attempted to examine the characteristics of reaction mechanisms. From these results we get the conclusion that non-compound processes play an important role in the reactions. Two features are characteristic of these processes : large cross-sections for charged particle emission and angular distribution of fission fragments closed to isotropy in the laboratory system.

In the energy range 25 to 45 MeV/nucleon, a comparison was made between the present results and those from an experimental study of α-particle induced reactions on ^{206}Pb. Also a comparison was made with an α-nucleus collision model applied to ^{206}Pb.

All the observations strongly suggest a breakup of the projectile ^{3}He followed by the interactions of the fragments with the target nucleus.

1. **Introduction.** — ^{3}He particles are an interesting projectile for the study of low-energy nuclear reactions. Stripping and pickup reactions, in particular, are of importance in nuclear spectroscopic studies because of the low binding energy of ^{3}He (7.7 MeV) and its tendency to form the more stable α-particle by neutron pickup. In a comparative study of reactions induced in heavy elements (A = 180-209) by ^{3}He and α-particles having energies up to 45 MeV Scott *et al.* [1] concluded that compound nucleus formation accounted for virtually the entire reaction cross-section in the case of the latter but not in that of the former. Direct processes, as manifested by the copious emission of charged particles, were found to be of importance for ^{3}He.

Golchert *et al.* [2], who studied the interactions of ^{3}He with Cu up to 70 MeV, arrived at similar

(*) Guggenheim Fellow, Institut de Physique Nucléaire, Orsay, France, 1971-72.

conclusions. Other reaction studies with ^{3}He include those of Hofstetter and Stickler [3], who studied the ^{209}Bi(^{3}He, xn)$^{212-x}$At reactions up to 70 MeV and Hermes *et al.* [4], who studied the ^{197}Au(^{3}He, xn) reactions up to 70 MeV. In this second work the excitation functions were compared with the spin-dependent statistical theory. The calculation could not reproduce the high-energy tails of the excitation functions.

All the research of this type that has been published to date is restricted to ^{3}He bombarding energies below 80 MeV. It appeared to us of interest to examine the situation at higher energies and in this article we present the results of a study of the reactions induced in ^{206}Pb by ^{3}He ions having energies between 80 and 205 MeV. We have measured the excitation functions of the ^{206}Pb(^{3}He, xn)$^{209-x}$Po reactions for x = 3-14 and those of the (^{3}He, pxn) reactions for x = 2-5. Angular distributions of fission fragments were measured at 100, 125, 150, and 175 MeV and total fission cross-sections at these energies were obtained from the data.

On the basis of these results we have attempted to examine the characteristics of the principal mechanisms in the interaction of ^{3}He with heavy elements : compound and non-compound processes, characteristics of fission, importance of charged particle emission.

The reactions of ^{206}Pb with α-particles of comparable energies to those used in the present work have been previously studied by Bimbot and Le Beyec [5]. It is of interest to compare the results of these two studies in order to determine if the effects of the difference in ^{3}He and ^{4}He binding energies noted at low energies persist at higher energies.

There are no well developed theoretical models with which to confront the experimental data for the energies of present interest. At lower energies, the precompound model of Griffin [7] as developed by Blann [8, 9] has been successful but it has been shown [5, 6] that this model cannot account for the ^{206}Pb(α, xn) reaction cross-sections above 80 MeV. Gabriel *et al.* [10] developed a model to represent the interaction of high-energy complex projectiles with nuclei. In this model the projectile is treated as a collection of nucleons each of which interacts separately by a series of quasi-free collisions subject to the restriction that the nucleons are spatially correlated at the initial point of impact. This model has been applied to the system ^{206}Pb + α between 100 and 260 MeV. The comparison with the ^{206}Pb + ^{3}He reactions offers an opportunity to present the results of these calculations.

2. **Experimental procedure.** — The experiments were performed with the external ^{3}He beam of the Orsay synchrocyclotron, whose energy is 210 MeV. Copper absorbers mounted on the apparatus described in ref. [11] were used to degrade the beam energy down to 80 MeV. Energy losses were calculated on the basis of the tables of Williamson *et al.* [12]. The uncertainty in energy is estimated as ± 1 MeV at the maximum energy, increasing on account of straggling to ± 3 MeV at 100 MeV.

2.1 (^{3}He, xn) REACTIONS. — The polonium isotopes formed in (^{3}He, xn) reactions are listed together with their pertinent decay properties in table I. The half-lives of these nuclides range from 8.8 days to 2 seconds. This wide range in half-lives led us to employ two different techniques for the determination of the cross-sections.

TABLE I

Decay properties of polonium isotopes [26]

Isotope	$T_{1/2}$	E_α MeV	α-branching ratio (%)	Desintegration mode
—	—	—	—	—
^{206}Po	8.8 d	5.22	5.45	
^{205}Po	1.8 h	5.25	0.07	^{205}Bi-γ (1.76 MeV) 27 % (15.3 d)
^{204}Po	3.6 h	5.38	0.75	
^{203m}Po	29 mn	5.37	0.11	^{203}Pb-γ-280 keV 81 % (52 h)
^{202}Po	45 mn	5.57	2	
^{201m}Po	9 mn	5.77	2.9	
^{201}Po	15.8 mn	5.67	1.15	
^{200}Po	11.4 mn	5.85	12.2	
^{199m}Po	4.1 mn	6.04	27.5	
^{199}Po	5.2 mn	5.93	2.6	
^{198}Po	1.7 mn	6.16	57	
^{197m}Po	26 s	6.38	100 (*)	
^{197}Po	54 s	6.29	100 (*)	
^{196}Po	5.5 s	6.53	100 (*)	
^{195m}Po	2 s	6.71	100 (*)	
^{195}Po	4.5 s	6.62	100 (*)	

(*) Adopted value.

2.1.1 The cross-sections for the (^{3}He, xn) reactions for x = 3-10, corresponding to the formation of ^{206}Po-^{199}Po, were determined by the activation method. The targets consisted of lead foils, enriched to 99.8 % in ^{206}Pb, with a thickness of 10 mg/cm^2. The beam intensity was determined with a Faraday cup. Six irradiations were performed ; the bombarding energies were 85, 100, 115, 135, 170 and 205 MeV. Following irradiation the targets were dissolved in nitric acid and Po was separated by spontaneous deposition on silver foil, a technique that has been described elsewhere [13]. Five successive depositions were required in order to completely extract the polonium. The radioactive decay of the various isotopes was measured either by α-spectroscopy or by measurements of γ-rays emitted in the decay of the corresponding bismuth decay products.

2.1.2 The light polonium isotopes have half-lives that are too short for the type of measurement described above. We have used the helium jet technique [14] for the measurement of the activities of ^{201}Po-^{195}Po (x = 8-14). Relative excitation func-

tions for these products were measured between 80 and 205 MeV. The yields of ^{201m}Po, ^{200}Po and ^{199m}Po were measured by both techniques permitting the helium jet data to be converted to absolute cross-sections.

The helium jet apparatus used in our experiment has been described elsewhere [15]. Its use with light ion beams from the synchrocyclotron poses some special problems. These arise from the fact that even at the highest bombarding energy, 205 MeV, the recoil energy of a ^{209}Po compound nucleus is only 2.9 MeV. The range of a Po nucleus of this energy in the target material is only 0.39 mg/cm^2, which is less than the target thickness (0.52 mg/cm^2). As a result, only a fraction of the reaction products recoil out of the target. We have applied a correction for the energy dependence of this effect on the assumption of full momentum transfer by assigning to each target an effective thickness equal to the recoil range at that particular bombarding energy. The results obtained in this fashion at 100 MeV were normalized to the data obtained by the activation method in the manner outlined above. As we shall see later, the assumption of a full momentum transfer can be invalid for the high energy part of the excitation functions. However up to $x = 10$ the corrected cross-sections are not in strong disagreement with the activation results. For $x \geqslant 11$ the high energy tail can be underestimated because of this correction for effective target thickness.

In order to avoid a rather high detector background with the beam on, the activity measurements were performed while the beam was off. The experiments thus consisted of a series of alternate irradiation and counting periods of equal duration. Two types of cycles were used in order to accommodate the expected range in half-lives : 10 s-10 s and 2 s-2 s. The alternation between irradiation and counting periods was controlled electronically [16]. Since the half-lives of the products of interest were comparable or longer than the cycle time only a fraction of the nuclides reaching the collector decayed during counting periods. The number of nuclides produced was obtained from the number detected in terms of the irradiation or counting time, τ, the decay constant of a given nuclide, λ, and the number of cycles, n, by the relation

$$\frac{N_{\text{produced}}}{N_{\text{observed}}} = \frac{n\lambda\tau}{(1 - e^{-\lambda\tau})^2 \sum_{j=0}^{n-1} (n - j)\, e^{-2j\lambda\tau}}.$$

In the helium jet experiments the beam intensity was determined by means of a calibrated helium ionization chamber.

2.2 (^{3}He, pxn) Reactions. — These reactions lead to bismuth isotopes. After the extraction of polonium from the dissolved target as described above bismuth is left in solution. The solutions were directly assayed with a Ge(Li) detector having a resolution of 2.7 keV at 1.33 MeV. ^{205}Bi and ^{206}Bi were detected by their characteristic γ-rays (see table II). Corrections were applied for the electron capture decay of the corresponding Po nuclides prior to the Po-Bi separation as described in ref. [5]. In the case of ^{203}Bi the observed γ-ray was that of the ^{203}Pb daughter so that the measured yield corresponds to the sum of the (^{3}He, p5n) and (^{3}He, 2p4n) reactions.

TABLE II

Decay properties of bismuth isotopes [27]

Isotope	$T_{1/2}$	E_γ MeV	Desintegration mode	Photons/ Desintegration %
^{206}Bi	6.24 d	1.720	electron capture	36
^{205}Bi	15 d	1.766	electron capture	27
^{203}Bi	11.8 h		electron	
↓				
^{203}Pb	52.1 h	0.279	capture	81

2.3 Fission of ^{206}Pb. — Angular distributions of fission fragments were determined at 100, 125, 151 and 175 MeV. A 0.5 mg/cm^2 thick ^{206}Pb (95 % enrichment) target was irradiated in a 16 cm diameter vacuum chamber by a collimated ^{3}He beam. Fission fragments were detected in muscovite mica foils mounted along the inner wall of the chamber at a 30° angle to the horizontal. A schematic diagram of the apparatus is shown in figure 1. A faraday cup located at the exit of the chamber was used to determine the beam intensity.

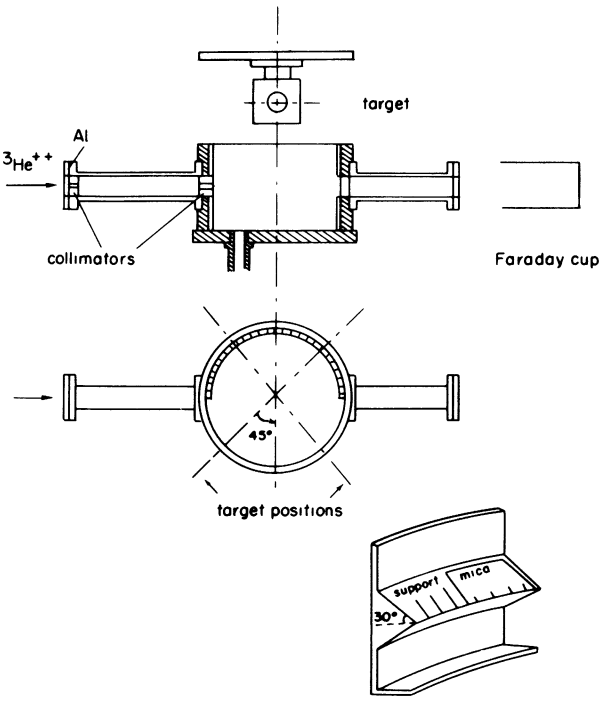

Fig. 1. — Schematic diagram of irradiation chamber and mica foil supports.

The mica detectors were treated with a 48 % HF solution in order to develop the fragment tracks. Background tracks in the mica could be distinguished since the foils had been overdeveloped prior to irradiation. The mica foils were scanned with an optical microscope.

3. **Results.** — The measured cross-sections of the (^{3}He, xn) reactions are tabulated in table III. The results obtained by the helium jet method are marked with an asterisk. The excitation functions are presented in figures 2-4 for x = 3-6, x = 7 and 8, and x = 9-14, respectively. The cross-sections of the (^{3}He, pxn) reactions are listed in table IV and the excitation functions shown in figure 5.

The angular distributions of fission fragments for 151 and 175 MeV ^{3}He ions were measured between 10° and 170° in two separate irradiations at each

TABLE III

Cross-sections of ^{206}Pb(^{3}He, xn) *reactions.*
*Values with * are obtained with* He-*Jet technique*

E MeV	Cross-sections mb															
	^{206}Po	^{205}Po	^{204}Po	^{203m}Po	^{202}Po	^{201m}Po	^{201}Po	^{200}Po	^{199m}Po	^{199}Po	^{198}Po *	^{197m}Po *	^{197}Po *	^{196}Po *	^{195m}Po *	^{195}Po *
85	5.9 ±1.9	29 ±3	52 ±15.5	86.6 ±11.3	113.6 ±20	157 ±32	144 ±30	192 ±32 168 ±40*	32 ± 7 19.3± 4.8*	26 ± 8						
90						186 ±46*		179.4±44*	50 ±12*							
95								145 ±36*	46.6±11*		1.1 ±0.3					
100				71 ±10	76.6 ±23	128.7±35 120 ±30*	76.5 ±25	123 ±27 126.3±31*	93 ±17 104.5±26*	60 ±15	4.1 ±1					
105								157 ±39*	108.7±27*		11.2 ±2.8		0.11 ±0.03			
110						107.6±27*		114 ±28*	102 ±25*		17 ±4.3	0.23 ±0.06	0.13 ±0.03			
115	4.20 ±0.60	20.5 ±2	25.3 ± 8	53 ± 7	56.6 ±10	77.5±17	64.6 ±17	90 ±19 108 ±27*	84 ±15 88.3±22*	43.2 ±13	21.8 ±5.5	2 ±0.5	0.39 ±0.10			
120						52 ±13*		74 ±18*	65.6±16*		21 ±5.3	2.33 ±0.6	0.29 ±0.10			
125								92.4±23*	71.6±18*		27.6 ±6.9	6 ±1.5	1.25 ±0.30	0.31 ±0.08		
130						48 ±12*		63 ±16*	61.3±15*		25.6 ±6.4	7.30 ±1.8	1.00 ±0.20			
135				34.5 ± 5	46 ±13	59.1±15	51 ±13	63 ±12 55.4±14*	54 ±12 43.7±11*	31.5 ± 8	18.6 ±4.6	8.50 ±2.1	1.44 ±0.40	1.27 ±0.30		
140								38.6± 9.6*	44.8±11*		18.6 ±4.6	9.00 ±2.3	1.23 ±0.30	1.47 ±0.40	0.023 ±0.005	0.03 ±0.01
145								45 ±11*	35.2± 8.8*		14.3 ±3.6	8.30 ±2	0.81 ±0.20	2.70 ±0.70		
151								29.5± 7.3*	38.5± 9.6*		16.8 ±4.2	9.60 ±2.4	0.93 ±0.20	4.00 ±1	0.174 ±0.040	0.08 ±0.02
153								34.7± 8.6*	30.8± 7.7*		13.2 ±3.3	7.90 ±1.9	1.03 ±0.30	3.50 ±0.90		
159								32.2± 8*	28 ± 7*		11.9 ±2.9	7.00 ±1.8	1.22 ±0.30	3.00 ±0.80	0.530 ±0.10	0.10 ±0.02
164								30.4± 7.6*	27.5± 6.9*		11.3 ±2.8	6.00 ±1.5	0.72 ±0.20	2.94 ±0.80		
170	3.30 ±0.40	14.3 ±1.5	8.30 ± 2.3	21 ± 3	14.3 ± 3.2	16.8± 4	17 ± 4	21 ± 4.4	21 ± 4	11.6 ± 4.2		6.80 ±1.7		3.20 ±0.80	0.918 ±0.20	0.11 ±0.02
174								17.2± 4.3*	14.6± 3.6*		6.9 ±1.7	3.80 ±1	0.72 ±0.20	2.10 ±0.50		
185								21.8± 5.5*	19 ± 4.7*		8.2 ±2	5.30 ±1.3	0.96 ±0.20	2.75 ±0.70		
190						10 ± 2.5*								2.80 ±0.70	0.875 ±0.20	0.12 ±0.02
195								13 ± 3.2*	9.3± 2.3*		4.6 ±1.2	3.00 ±0.8	0.58 ±0.20	1.63 ±0.40		
205				6.8 ± 1	6.3 ± 1.7	6.9± 2.2	6.5 ± 2.5	10 ± 2.2 10 ± 2.5* 11.3± 2.8*	8 ± 1.5 10.1± 2.5* 7.3± 1.8*	6 ± 1.8	3.8 ±0.9 4.8 ±1.2	2.50 ±0.6 3.10 ±0.7	0.52 ±0.10 0.50 ±0.10	1.51 ±0.40 1.51 ±0.40	0.65 ±0.20	0.12 ±0.02

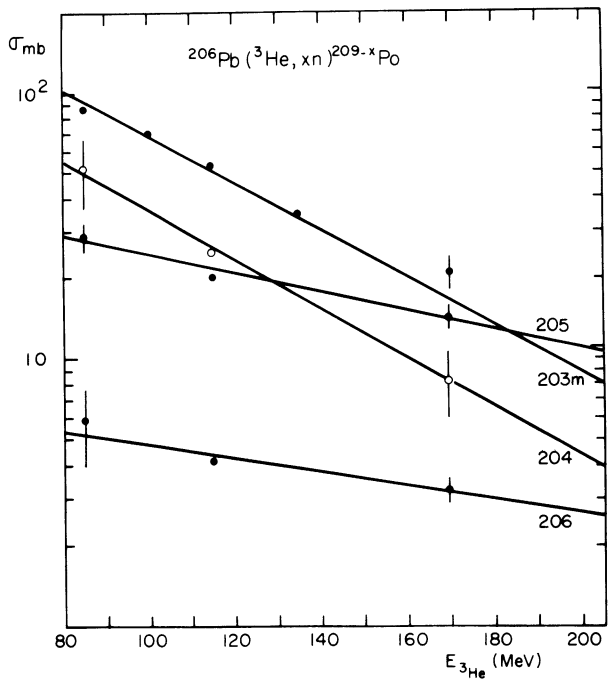

FIG. 2. — Excitation functions for ^{206}Pb(^{3}He, xn) reactions for x = 3-6.

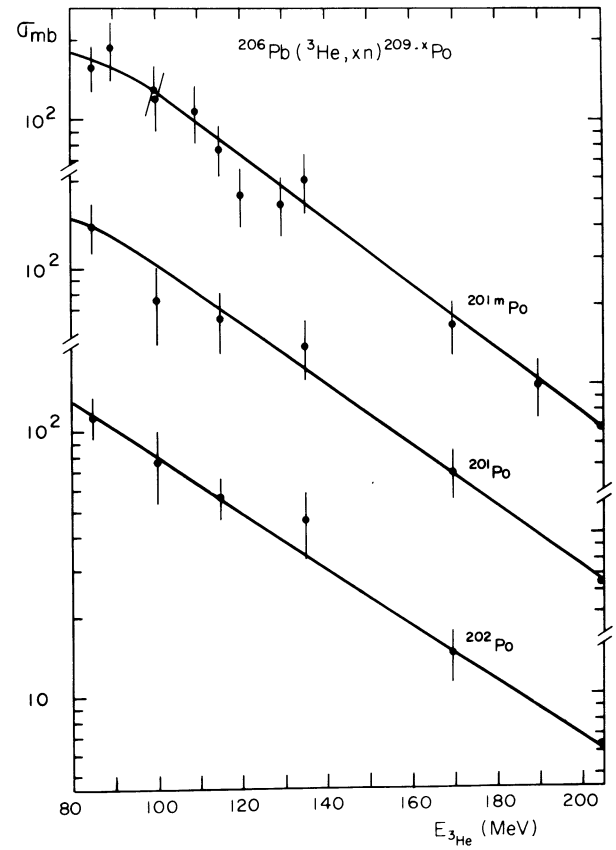

FIG. 3. — Excitation functions for ^{206}Pb(^{3}He, xn) reactions for x = 7 and 8.

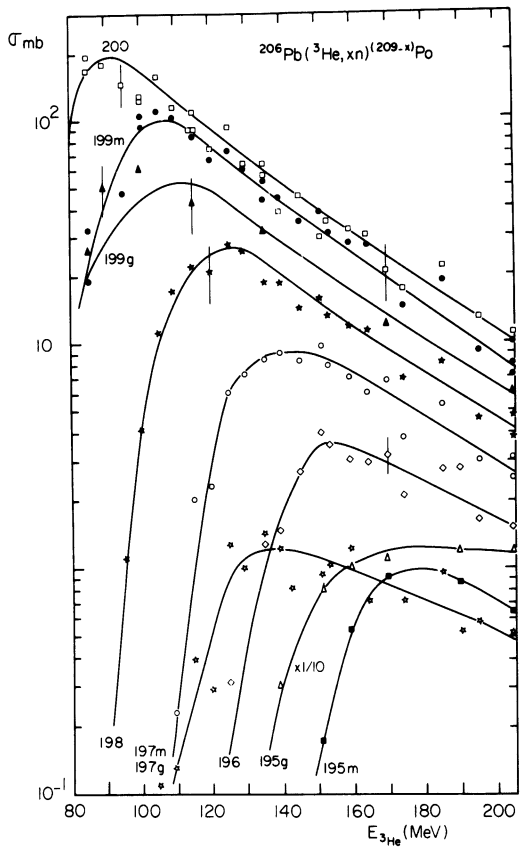

FIG. 4. — Excitation functions for ^{206}Pb(^{3}He, xn) reactions for x = 9-14.

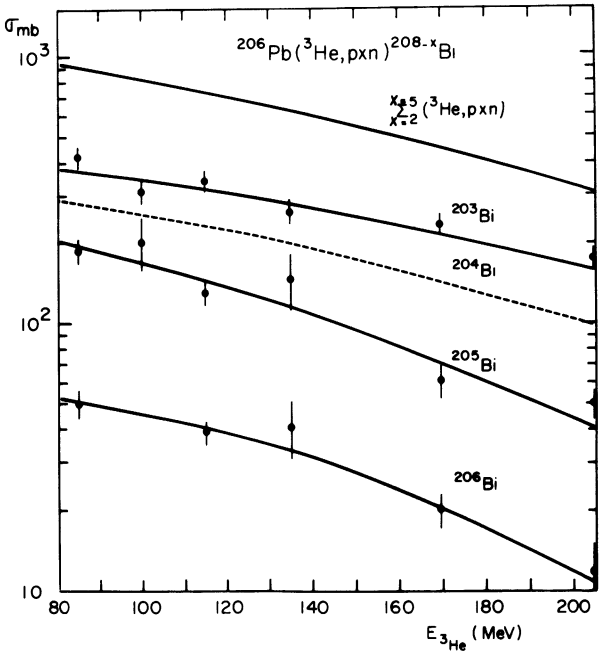

FIG. 5. — Excitation functions for ^{206}Pb(^{3}He, pxn) reactions for x = 2-5. Curve for x = 4 is estimated.

TABLE IV

Cross-sections of $^{206}Pb(^{3}He, pxn)$ reactions

E MeV	Cross sections mb $^{206}Pb(^{3}He, p2n)^{206}Bi$	$^{206}Pb(^{3}He, p3n)^{205}Bi$	$^{206}Pb(^{3}He, p5n)^{203}Bi$
85	50 ± 5.5	188 ± 20	418 ± 38
100		204 ± 45	310 ± 31
115	39 ± 4	131 ± 14	341 ± 31
135	41 ± 10	147 ± 34	263 ± 26
170	19.5 ± 2.8	61 ± 8	234 ± 21
205	12.3 ± 3	56 ± 12	175 ± 17

energy. The curves are somewhat asymmetric with a maximum in the forward direction in the laboratory (L) system. The distributions in the center of mass (C.M.) system were obtained by means of the relation :

$$\theta_{C.M.} = \text{arc sin } (\overline{X} \sin \theta_L) + \theta_L$$

where $\theta_{C.M.}$ and θ_L are, respectively, the angles in the two systems.

The parameter $\overline{X}$ is defined as $\overline{X} = V_R \mid V_f$ where V_R is the mean recoil speed of the fissioning nucleus and V_f is the mean speed of a fission fragment in the C.M. system. This parameter was adjusted to yield angular distributions symmetric about 90° in the C.M. system. This condition was met at both energies with $\overline{X} = 0.02$. At bombarding energies of 100 and 125 MeV, where experimental data were only obtained between 90° and 170°, the same $\overline{X}$ value was used in making the transformation.

The ratio of differential cross-sections in each of the two systems is given by the usual expression [17] :

$$\left(\frac{d\sigma}{d\Omega}\right)_{C.M.} \Big/ \left(\frac{d\sigma}{d\Omega}\right)_{L} = \frac{1 + \overline{X} \cos \theta_{C.M.}}{(1 + \overline{X}^2 + 2\,\overline{X} \cos \theta_{C.M.})^{3/2}} .$$

The C.M. angular distributions at 100 and 175 MeV are displayed in figure 6. Integration of the angular distributions yields the total fission cross-sections and these are summarized in table V. The excitation function of the $^{206}Pb(^{3}He, f)$ reaction is shown in figure 7.

TABLE V

Cross-sections for fission of ^{206}Pb by ^{3}He

E MeV	100	125	150	175
σ_{mb}	640 ± 45	867 ± 60	832 ± 50	938 ± 65

4. **Discussion and interpretation.** — 4.1 (^{3}He, xn) REACTIONS. — It is of interest to point out the persistence at high energies of reactions involving the emission of only a few neutrons. The (^{3}He, 3n or 4n) reactions are thus observed at 200 MeV (Fig. 2) with cross-sections of several millibarns. In general, even for $x > 8$, the excitation functions invariably

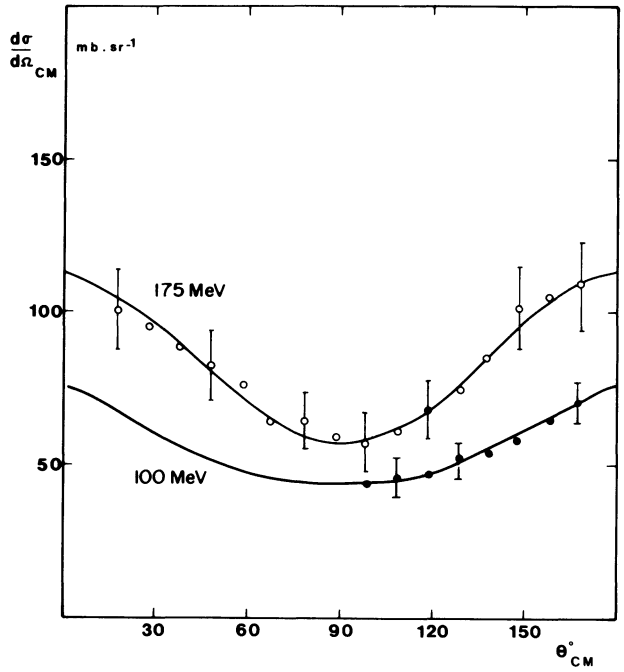

FIG. 6. — Angular distribution of fission fragments from the $^{206}Pb(^{3}He, fission)$ reaction at 100 and 175 MeV.

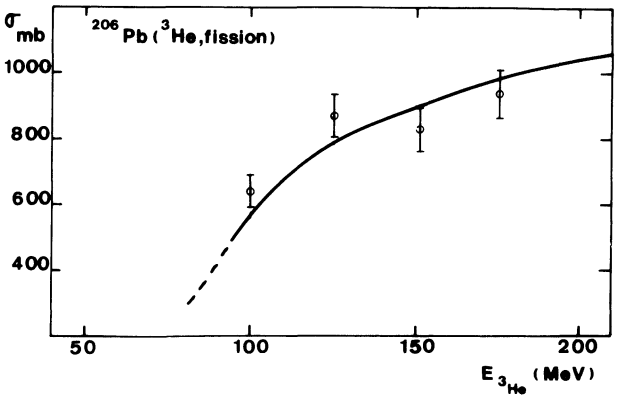

FIG. 7. — Excitation function for $^{206}Pb(^{3}He, fission)$.

have a high-energy tail (Fig. 4) that cannot be accounted for by a compound nuclear mechanism.

The general behaviour of the (^{3}He, xn) reactions is similar to that observed for the (α, xn) reactions [5]. However, the latter display a faster exponential dropoff in cross-section. It can also be seen that the areas under the excitation functions decrease rapidly with increasing x reflecting the increasing importance of other decay channels, such as charged particle emission and fission.

4.2 (^{3}He, pxn) REACTIONS. — Our results are rather limited since x only varies between 2 and 5. The curves in figure 5 represent the high-energy tails of the excitation functions. The compound nuclear contribution to these reactions occurs below 80 MeV. The cross-sections vary relatively little between 80 and 200 MeV. It can be noted that the cross-sections of the (^{3}He, pxn) reactions are larger than those of the (^{3}He, (x + 1) n) reactions, for which the same number of nucleons is emitted. We shall return to this point further on.

4.3 (^{3}He, FISSION) REACTION. — If one assumes that fission occurs following compound nucleus formation and is thus accompanied by full momentum transfer, and if one further assumes that the velocity of the fissioning nucleus is equal to that of the compound nucleus, we can estimate the value of the parameter $\overline{X}$, defined above. This parameter is given by the expression

$$\overline{X} = \left[\frac{EmM_f}{M_{CN}^2 E_f}\right]^{1/2}$$

where E is the kinetic energy of the incident particle of mass m, M_{CN} is the mass of the compound nucleus, and M_f and E_f are, respectively, the mean mass and mean C.M. kinetic energy of the fission fragments. In the energy range of present interest both the mass and kinetic energy distributions of the fragments are essentially symmetric. We use a value of 150 MeV [18] for the total kinetic energy (2 E_f) released in fission and assume that the mass of the fissioning nucleus is close to that of the compound nucleus so that $M_f \simeq 1/2\ M_{CN}$. Under these conditions $\overline{X}$ ranges from 0.10 to 0.13 for incident energies between 100 and 175 MeV. The value of $\overline{X}$ determined experimentally from the angular distribution at 175 MeV is only 0.02, substantially smaller than that calculated on the basis of compound nucleus formation. This comparison indicates that the fissioning nucleus has, on the average, only a small recoil momentum. Evidently, fission following compound nucleus formation accounts for at most a small fraction of the fission cross-section although, of course, fission may still be an important decay channel in compound nuclear reactions. The results are consistent with a mechanism in which direct or precompound particle emission carries off most of the linear momentum of the projectile, with fission occurring in a subsequent step.

4.4 CONTRIBUTION OF DIFFERENT TYPES OF REACTIONS. — We present in figure 8 the cross-sections of the ^{3}He-induced reactions regrouped by reaction type :

— curve (1) $\sum_{x=3}^{14}$ (^{3}He, xn) is the sum of the experimental (^{3}He, xn) reaction cross-sections ;

— curve (2) $\sum_{x=2}^{5}$ (^{3}He, pxn) has the same meaning for reactions involving the loss of a single charge. We recall that for $x = 5$ we have in fact obtained the sum of the (^{3}He, p5n) and (^{3}He, 2p4n) cross-sections. The curve for $x = 4$ was estimated (see Fig. 5) ;

— curve (3) represents the experimental fission cross-section.

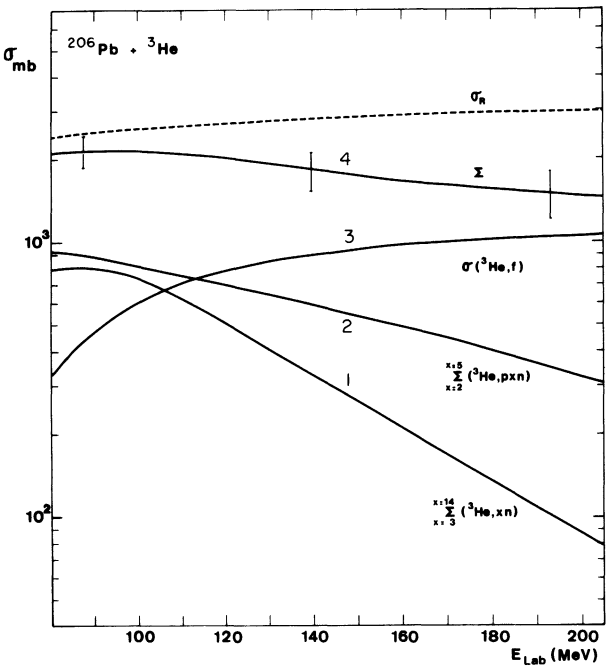

FIG. 8. — Contribution of different types of reactions to the ^{206}Pb + ^{3}He system.

The sum of these curves is given by the curve designated [4] where the error bars are an estimate of the experimental uncertainties. This sum curve may be compared with the total reaction cross-section, given by the curve labelled σ_R. The latter was obtained by the sharp cutoff model :

$$\sigma_R = \pi R^2 \left(1 - \frac{V}{\overline{E}}\right)$$

where V is the coulomb barrier, $\overline{E}$ the C.M. bombarding energy, and the radius R is taken as

$$R = R_{^3He} + 1.45\, A^{1/3}$$

where $R_{^3He}$ = 1.77 fm, as is the case for the α-particle [19]. This curve differs little from that calculated up to 50 MeV by means of the optical model by

Huizenga and Igo [19] for α + ^{206}Pb. At substantially higher energies one might expect the calculated curve to overestimate the value of σ_R because of the effect of nuclear transparency. One can estimate the magnitude of this effect by reference to the Monte Carlo calculation of Bertini [23] which is mentioned in this article. This calculation shows that the transparency of ^{206}Pb for 150 MeV incident α-particles is approximately 7 %. In view of the uncertainty in the experimental sum curve (curve 4 in Fig. 8) it is not worth including such an effect in the estimation of σ_R.

We observe that the experimental and calculated σ_R curves are in good agreement at the lowest energy but that the former falls increasingly short of the latter with increasing ^{3}He energy. This discrepancy must reflect the effect of a number of reaction channels that are missing in curve (4). While the experimental (^{3}He, xn) reactions are quite complete the same cannot be said for reactions involving charged particle emission. The experimental data do not include the contribution of the (^{3}He, pxn) reactions for $x > 5$ as well as that of all reactions involving the loss of more than a single charge unit (except for (^{3}He, 2p4n)). On the basis of the results obtained at lower energies by Golchert *et al.* [2] it is apparent that these reactions must have large cross-sections. It may be noted that the discrepancy displayed in figure 8 becomes as large as 1 barn at 200 MeV. This value is indicative of the importance of reactions involving the loss of 1 or more charge units.

4.5 CONTRIBUTION OF COMPOUND NUCLEAR REACTIONS TO THE FORMATION OF RESIDUAL NUCLEI. — It is possible to estimate that fraction of the cross-section for compound nucleus formation which subsequently leads to the formation of residual nuclei by evaporation. The ^{209}Po* compound nucleus deexcites either by neutron or charged particle evaporation or by fission. The statistical model evaporation calculations of Silveira [20] and Le Beyec [21] yield the probabilities, P_n, of neutron evaporation from excited ^{209}Po as a function of excitation energy.

The curves that have been obtained yield the probability of evaporating x neutrons as a function of energy for different x values as well as the total probability of emitting only neutrons, P_n, or charged particles as well ($P_c = 1 - P_n$). These results have been applied to the present data in the following three steps.

For each experimental (^{3}He, xn) excitation function, after adjustment in energy and normalization of peak amplitude, one can extract the contribution of the compound nuclear mechanism. The analysis made for x = 8-14 leads to the curves in figure 9. On the basis of the calculation of (α, xn) cross-sections by Bimbot and Le Beyec [5] it appears that this normalization procedure is reasonable since the precompound contribution only becomes of significance at energies corresponding to those beyond the peaks in the excitation functions. To be sure, this calculation

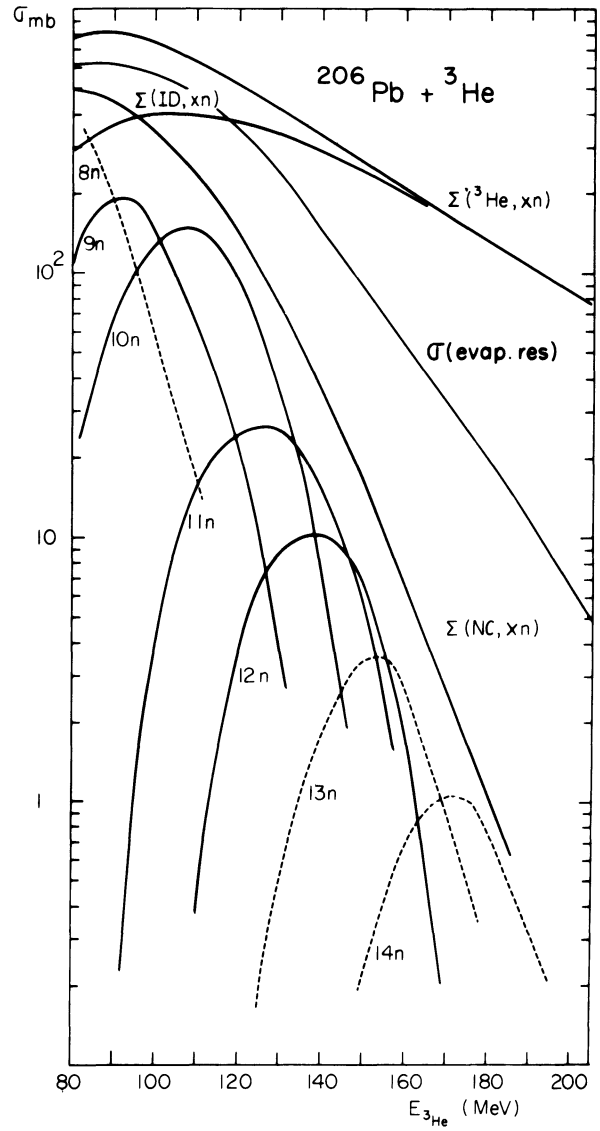

FIG. 9. — Contribution of compound nuclear mechanism to (^{3}He, xn) reactions. Curves for x = 13 and 14 are estimated.

was only performed up to x = 8 but one does not expect a qualitative difference for larger x values or ^{3}He projectiles. It should also be mentioned that the calculated curves are based on a spin independant approximation. Calculations in which angular momentum effects are included [4] yield somewhat less symmetric excitation functions and thus a slightly higher contribution of the compound nucleus mechanism at the highest energies.

The sum of these individual curves leads to the curve labelled $\sum$ (CN, xn), which corresponds to the fraction of the compound nucleus formation cross-section involving evaporation of only neutrons.

These cross-sections are related to the actual CN formation cross-sections by the relation :

$$\sigma(\mathrm{CN}) = \frac{\sum (\mathrm{CN}, x\mathrm{n})}{P_n} + \sigma(\mathrm{CN}, \mathrm{f})$$

where σ(CN, f) is that part of the total fission cross-section involving the formation of a compound

nucleus. The measured fission cross-section includes these events as well as those involving a direct or precompound process. It was shown above that the latter account for the major fraction of the fission cross-section but it is not possible to quantitatively establish the relative contributions of these two processes. We content ourselves with deducing from the data the cross-section for the production of residual nuclei by evaporation, $\sigma(\mathrm{RE}) = \frac{\sum (\mathrm{CN}, xn)}{P_n}$. Figure 9 shows the curve obtained in this fashion. On the basis of the values of the total reaction cross-section (curve σ_R, Fig. 8) one can estimate that the probability of forming residual nuclei following compound nucleus formation decreases from ~ 20 % at 100 MeV to less than 1 % around 200 MeV.

We have represented by the curve labelled $\sum$ (DI, xn) in figure 9 the difference between $\sum$ (^{3}He, xn) and $\sum$ (CN, xn). It is seen that above 130 MeV the (^{3}He, xn) reactions are primarily formed by non-compound processes.

4.6 COMPARISON WITH THE ^{206}Pb(α, x) REACTIONS. — It is of interest to compare the curves in figure 8 with the corresponding results obtained for the interaction of ^{206}Pb with α-particles.

On the basis of the results of Bimbot *et al.* [5, 6] we show in figure 10 the summed excitation functions for the following different types of reactions : $\sum$ (α, xn) for x = 2-12 and $\sum$ (α, pxn) for x = 2-5. Note that these values of x are the same ones used to obtain the summed ^{3}He curves. The curve for $\sigma(\alpha$, fission) was obtained by Khodai-Joopari [22] up to 120 MeV.

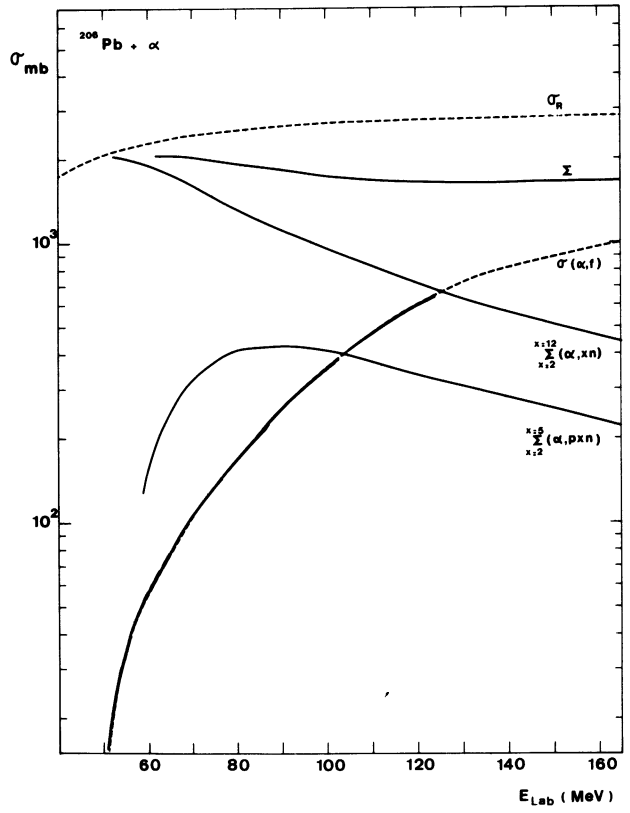

FIG. 10. — Contribution of different types of reactions to the ^{206}Pb + α system.

The comparison between the curves in figures 8 and 10 indicates some strong similarities as well as a number of specific differences. The curve for $\sum$ (α, xn) thus peaks in the vicinity of 50 MeV at which point it merges with the σ_R curve. By contrast, $\sum$ (^{3}He, xn) appears to peak around 80 MeV and does not amount to more than a third of σ_R. This result is in accord with the observation at lower energies [1, 2] that the competition of (^{3}He, Axn) reactions, where A is a charged particle, with (^{3}He, xn) reactions is very strong. Although qualitative, this conclusion expresses an important feature of ^{3}He-induced reactions.

If one wishes to attempt a more quantitative comparison between the reactions induced by α-particles and ^{3}He at high energies it is necessary to choose an appropriate comparison variable. Neither the kinetic energy of the incident particle nor the excitation energy appear to be appropriate choices since the compound mechanism is of minor importance. On the other hand, if one wishes to compare reactions involving direct processes the appropriate variable appears to be one related to the speed of the incident nucleons, such as the energy per nucleon of the projectile, E/A. In another connection, the use of this variable permits a comparison with an α-nucleus collision model developed by Gabriel, Santoro, and Alsmiller [10]. These authors assume that α-nucleus interactions can be simulated by the interaction of the 4 constituent nucleons with the nucleus. These nucleons interact independently of each other except for an initial spatial correlation at the point of entry. Specifically, the α-particle is treated as two p-n pairs separated by a fixed distance. Each nucleon has an energy $(E_\alpha - B)/4$ where E_α is the energy of the incident α-particle and B is the α binding energy (~ 28 MeV). Nucleons that penetrate into the nucleus can initiate intranuclear cascades which can be simulated by the Monte Carlo code of Bertini [23]. The deexcitation of the residual nuclei by evaporation is calculated by means of the code of Dresner [24] and Guthrie [25].

This model was applied to the interaction of ^{206}Pb with α-particles of 100, 140, and 180 MeV. The comparison between ^{206}Pb + ^{3}He, ^{206}Pb + α, and calculation was made over the common energy domain of 25-45 MeV/nucleon in terms of summed cross-section curves, $\sum$ (A, xn) for x = 3-12 and $\sum$ (A, pxn) for x = 2-5. The results are shown in figure 11.

The most striking observation is the already noted importance of the (^{3}He, pxn) reactions relative to the (α, pxn) reactions. At a given energy per nucleon the ratio of their cross-sections is in the vicinity of 3 over the entire range of energies covered in this comparison. One can think of a variety of processes in which the weakly bound ^{3}He can be split into d + p with the direct emission of one or the other of these particles. The complementary particle pene-

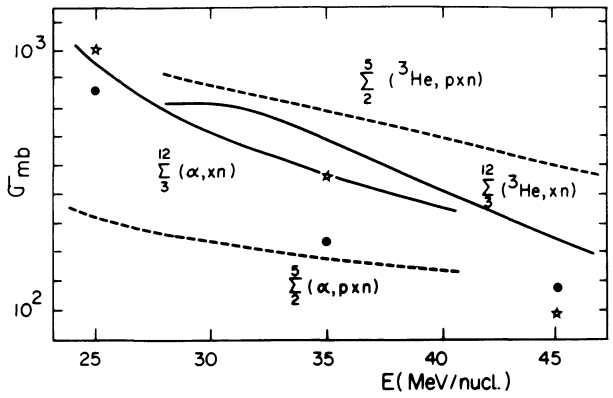

FIG. 11. — Comparison of (xn) and (pxn) reactions induced in ^{206}Pb by ^{3}He- and α-particles. * — Calculated (α, xn) cross-sections for x = 7-12 from ref. [10]. • — Similar calculation for (α, pxn) reactions for x = 2-5.

trates the struck nucleus and either forms an excited intermediate nucleus or leads to a direct reaction. This type of process will favor the (^{3}He, pxn) reactions over (^{3}He, xn) or (^{3}He, ypxn) reactions. In contrast to the mechanism presumed to occur in ^{3}He reactions, the α-particle necessarily will behave in a more collective fashion because of its greater binding energy. Proton emission resulting from α breakup is much less probable in this case and the (α, pxn) reactions are, in fact, more likely to involve (α, p) collisions in the nucleus [5].

Gabriel *et al.* [10] have noted that their model is based on a rather simplified picture of the interaction, one that is most valid at high energies. Some of the features of the model, such as the intranuclear cascade, do not appear to be physically justifiable at energies below 40-45 MeV per nucleon. The results obtained from this model for the (α, pxn) reactions appear to confirm these limits of applicability since one notes a factor-of-two discrepancy from the experimental data at low energies and a satisfactory agreement starting at 40 MeV per nucleon. It should be noted again that this comparison only applies to the (α, pxn) reactions for x = 2 to 5 whereas at the energies of present interest larger x are possible. However, there are no experimental data available for a more extensive comparison.

If one now turns to a comparison of the (^{3}He, xn) and (α, xn) reactions it is apparent that the sum of the cross-sections for x = 3-12 is nearly independent of projectile between 25 and 45 MeV per nucleon. If one examines the respective excitation functions, the ^{3}He results in figure 9 and the α results in figure 9 of reference [5], it is evident that at these energies the cross-sections come from the high-energy tails and can thus be attributed to non-compound processes. The reactions involving exclusively neutron emission are thus quite similar for ^{3}He and ^{4}He. The initial capture of a neutron by ^{3}He followed by direct (α-n) interactions and subsequently by neutron evaporation could explain this similarity. The agreement with the calculated $\sum$(α, xn) cross-sections appears to be satisfactory, particularly at low energies. This agreement is unfortunately more apparent than real since the calculation predicts that for x = 3-6 the cross-sections should be negligibly small while experimentally these reactions account for nearly half the (α, xn) yield at low energies. Furthermore, the calculated points suggest a linear decrease in cross-sections with energy. This dropoff is too fast and shows that the model does not adequately account for the (α, xn) reactions at high energies.

An important drawback of the calculation by Gabriel *et al.* [10] is that these authors do not take fission into account even though this process constitutes an important decay mode. The calculated results should thus be corrected for this effect but we have no way of estimating how this correction should be apportioned between the various types of reactions. One can predict, however, that the effect of fission will be larger on the (α, xn) than on the (α, pxn) cross-sections because the fission barrier is smaller for polonium isotopes than for the corresponding bismuth isotopes.

5. **Conclusion.** — In the course of this work we have examined the interaction of 80-200 MeV ^{3}He ions with a heavy element. The experimental results obtained for the (^{3}He, xn), (^{3}He, pxn) and (^{3}He, fission) reactions show that non-compound processes are of dominant importance.

The direct mechanisms, which have already been observed at low energies, are even more important in the energy region of present interest. Two features are particularly characteristic of these processes. First, fission primarily involves the transfer of only a small fraction of the projectile momentum to the struck nucleus. Second, reactions involving charged particle emission are very important, accounting for ~ 2/3 of the reaction cross-section at 200 MeV with fission accounting for nearly all of the remaining 1/3. These observations strongly suggest a breakup of the projectile followed by the interaction of the fragments with the target nucleus. The low binding energy of ^{3}He favors such a breakup.

Reactions involving only neutron emission (^{3}He, xn) are of minor importance (~ 2 % of σ_R at 200 MeV) but do permit the attainment of high x values (x = 14 in the present work). One can see that in a mass region where fission is much less important, ^{3}He-induced reactions at high energies should be an effective way of producing very neutron deficient nuclides.

Acknowledgments. — We wish to thank M. Lefort for his interest in this work and for valuable discussions. The calculation of the ^{206}Pb + α reactions was performed at Oak Ridge National Laboratory by H. W. Bertini, R. L. Hahn and R. T. Santoro, whose cooperation is greatly appreciated. We are grateful to Cl. Deprun for his help with the experimental work and to the operating staff of the Synchrocyclotron for their assistance.

References

[1] SCOTT, N. E., COBBLE, J. W. and DALY, P. J., *Nucl. Phys. A* **119** (1968) 131.

[2] GOLCHERT, N. W., SEDLET, J. and GARDNER, D. G., *Nucl. Phys. A* **152** (1970) 419.

[3] HOFSTETTER, K. J. and STICKLER, J. D., *Phys. Rev. C* **9** (1974) 1064 and 1072.

[4] HERMES, F., JASPER, E. W., KURZ, H. E., MAYER-KUCKUK, T., GOUDSMIT, P. F. A. and ARNOLD, H., *Nucl. Phys. A* **228** (1974) 175.

[5] BIMBOT, R. et LE BEYEC, Y., *J. Physique* **32** (1971) 243.

[6] BIMBOT, R., JAFFREZIC, H., LE BEYEC, Y., LEFORT, M. et VIGNY-SIMON, A., *J. Physique* **30** (1969) 513.

[7] GRIFFIN, J. J., *Phys. Rev. Lett.* **17** (1966) 488.

[8] BLANN, M., *Phys. Rev. Lett.* **21** (1968) 1357.

[9] BLANN, M. and LANZAFAM, F. M., *Nucl. Phys. A* **142** (1970) 559.

[10] GABRIEL, T. A., SANTORO, R. T. and ALSMILLER, Jr. R. G., *Nucl. Sci. Eng.* **44** (1971) 104.

[11] TAKEUTCHI, F., CAMON, J. et YUASA, T., *Revue Phys. Appl.* **3** (1968) 281.

[12] WILLIAMSON, C. F., BOUJOT, J. P. et PICARD, J., Rapport CEA, R 3042 (1966).

[13] LE BEYEC, Y., Thesis Orsay (1966).

[14] MAC FARLANE, R. D. and GRIFFIOEN, R. D., *Nucl. Instrum. Methods* **24** (1963) 461.
MAC FARLANE, R. D., GOUGH, R. A., OAKEY, N. S. and TORGERSON, D. F., *Ibid* **73** (1969) 285.

[15] LE BEYEC, Y., LEFORT, M. and SARDA, M., *Nucl. Phys. A* **192** (1972) 405.

[16] Realized by E. Festa, Orsay.

[17] MICHALOWICZ, A., Cinématique des réactions nucléaires (Dunod) 1964.

[18] SIKKELAND, T., *Phys. Lett.* **31B** (1970) 453.

[19] HUIZENGA, J. R. and IGO, G., *Nucl. Phys.* **29** (1962) 462.

[20] DA SILVEIRA, R., Thesis Orsay (1965).

[21] LE BEYEC, Y. and LEFORT, M., *Nucl. Phys. A* **99** (1967) 131.

[22] KHODAI-JOOPARI, Univ. of California, Lawrence Radiation Lab., Repr. UCRL (1966) 16489.

[23] BERTINI, H. W., *Phys. Rev.* **188** (1969) 1171.

[24] DRESNER, L., ORNL, TM (1961) 196.

[25] GUTHRIE, M. P., ORNL (1969) 4379. ORNL, TM (1970) 3119.

[26] REYSS, J. L., Thesis 3^{e} cycle (1971) Orsay.

[27] *Nucl. Data Tables* **8** (1971) 445.